Distinct members of the *C. elegans* CeMbio reference microbiota exert cryptic virulence and infection protection

Xavier Gonzalez[1,2] and Javier E. Irazoqui[2]*

Affiliations:

[1]Immunology and Microbiology graduate program, Morningside Graduate School of Biomedical Sciences, University of Massachusetts Chan Medical School, Worcester MA 01605

[2]Department of Microbiology and Physiological Systems, University of Massachusetts Chan Medical School, Worcester MA 01605

*Corresponding author

Correspondence: javier.irazoqui@umassmed.edu

Abstract

Microbiotas are complex microbial communities that colonize specific niches in the host and provide essential organismal functions that are important in health and disease. A key aspect is the ability of each distinct community member to promote or

impair host health, alone or in the context of the community, in hosts with varied levels of immune competence. Understanding such interactions is limited by the complexity and experimental accessibility of current systems and models. Recently, a reference twelve-member microbiota for the model organism *C. elegans,* known as CeMbio, was defined to aid the dissection of conserved host-microbiota interactions. Understanding the physiological impact of the CeMbio bacteria on *C. elegans* is in its infancy. Here, we show the differential ability of each CeMbio bacterial species to activate innate immunity through the conserved PMK-1/p38 MAPK, ACh/WNT, and HLH-30/TFEB pathways. Using immunodeficient animals, we uncovered several examples of bacterial 'cryptic' virulence, or virulence that was masked by the host defense response. The ability to activate the PMK-1/p38 pathway did not correlate with bacterial virulence in wild type or immunodeficient animals. In contrast, ten out of twelve species activated HLH-30/TFEB, and most showed virulence towards *hlh-30*-deficient animals. In addition, we identified *Pseudomonas lurida* as a pathogen in wild type animals, and *Acinetobacter guillouiae* as avirulent despite activating all three pathways. Moreover, short pre-exposure to *A. guillouiae* promoted host survival of infection with *P. lurida,* which was dependent on PMK-1/p38 MAPK and HLH-30/TFEB. These results suggest that the microbiota of *C. elegans* is rife with "opportunistic" pathogens, and that HLH-30/TFEB is a fundamental and key host protective factor. Furthermore, they support the idea that bacteria like *A. guillouiae* evolved the ability to induce host innate immunity to improve host fitness when confronted with pathogens, providing new insights into how colonization order impacts host health.

Introduction

Animals exist as super-organisms, in association with complex and dynamic microbial communities known as the microbiota (Eberl, 2010; Kostic *et al.*, 2013; Peixoto *et al.*, 2020). Although awareness of the importance of animal microbiotas emerged decades ago (Marples *et al.*, 1970; Marples and Kligman, 1971; Shilov *et al.*, 1971), the local and systemic influences of the microbiota on host physiology have come into focus only in recent times (Huttenhower *et al.*, 2012; Peixoto *et al.*, 2020). Although examples of specific mechanisms of microbiota-host interaction have emerged (Kamada *et al.*, 2013; Gasaly *et al.*, 2021; Caballero-Flores *et al.*, 2023; Horrocks *et al.*, 2023), many aspects remain poorly understood. In particular, the functional significance of distinct microbiota members, in terms of their microbe-microbe and microbe-host interactions, is not fully understood. Due to the sheer size of such communities (in the order of thousands of species in humans (Wang *et al.*, 2017)) and to a dearth of information regarding the microenvironments within the host in which these communities assemble and interact, it is extremely challenging to develop a comprehensive understanding of microbe-microbe and microbiota-host interactions in health and disease. Smaller reference communities (Lawley *et al.*, 2012; Kostic *et al.*, 2013; Brand *et al.*, 2015) and simpler model organisms can be of assistance in understanding such fundamental principles and the evolutionary forces at play.

To fully understand the emerging properties of such complex microbial communities in interaction with the host requires moving beyond phenotypic potentials that are encoded in the individual assembled genomes and meta-genomes to actual

64 phenotypes, the expression of which is highly context-dependent. To develop a better
65 understanding of microbe-microbe and microbe-host interactions, one approach is to
66 define the phenotypic states of each microbiota member in isolation, within various
67 environments and including distinct host physiological states. Host mono-colonization is
68 frequently used as an approach to unravel host-microbiota interactions, including
69 interactions with the host's immune system (Geva-Zatorsky *et al.*, 2017; Rogala *et al.*,
70 2020; Weitekamp *et al.*, 2021). With current technologies, this problem quickly becomes
71 intractable due to the vast array of community members, the diverse potentials their
72 genomes encode, variable environments, and variation in host physiology across time
73 and space.

74 *Caenorhabditis elegans* is an invertebrate model organism that associates with a
75 much simpler intestinal microbiota than vertebrates, yet presents an innate immune
76 system that is by and large conserved in higher organisms (Irazoqui *et al.*, 2010b;
77 Harding and Ewbank, 2021). Conserved signaling pathways, including the PMK-1/p38
78 MAPK, ACh-WNT, and HLH-30/TFEB pathways, connect the presence of pathogenic
79 bacteria (or the damage they cause) with the induction of host defense genes that are
80 also evolutionarily conserved (Irazoqui *et al.*, 2010a; Visvikis *et al.*, 2014; Labed *et al.*,
81 2018; Fletcher *et al.*, 2019). Although much has been accomplished to reveal and
82 understand these pathways in the context of clinically relevant bacterial infections (e.g.,
83 *Pseudomonas aeruginosa, Enterococcus faecalis,* and *Staphylococcus aureus*) their
84 roles in interactions with the microbes that *C. elegans* encounters in the wild and that
85 constitute its natural microbiota have been largely unaddressed. The simplicity and
86 ease of experimental manipulation of the model enables a reductionist approach to

87 investigate microbe-microbe and microbe-host interactions in the whole, live organism.

88 Despite recent progress, much is unknown about the resident intestinal microbiota of
89 *C. elegans,* in terms of its members, their interactions within the community, and their
90 effects on host physiology and behavior. Recent groundbreaking studies have revealed
91 mechanisms by which the microbiota affects host metabolism, gene expression, and
92 behavior (Berg *et al.*, 2016; Berg *et al.*, 2019; Ortiz *et al.*, 2021; Taylor and Vega, 2021;
93 Obeng *et al.*, 2023). However, which microbiota members are beneficial or harmful to
94 the host under different environmental conditions remains poorly defined. To aid in
95 answering such fundamental questions, a consortium of *C. elegans* researchers defined
96 a minimal reference microbiota, named CeMbio, which comprises twelve representative
97 species of bacteria from various clades that are frequently found in association with the
98 wild *C. elegans* intestinal epithelium (Dirksen *et al.*, 2020). How these microbiota
99 members interact with the host's innate immune system and how they affect each other
100 is not well defined.

101 To address these knowledge gaps, we determined the ability of each CeMbio
102 member to activate three important host defense pathways, namely the PMK-1/p38
103 MAPK, ACh-WNT, and HLH-30/TFEB pathways, and to cause disease in animals that
104 lacked them. We identified a broad range of phenotypes both in terms of pathway
105 reporter gene induction and virulence in wild type and immunodeficient animals.
106 Furthermore, we identified a frank pseudomonad pathogen and an immunity-promoting
107 Acinetobacter species, which demonstrated immune-mediated antagonism against the
108 former. These microbe-microbe interactions suggest that the order of host colonization

may be critical to host health. These seminal discoveries set the foundation for further in-depth investigation of the mechanisms that mediate “cryptic” virulence, or virulence that is masked by the host immune response, and “Third-Party” microbe-microbe interactions that are mediated through the host’s immune system.

Experimental Results

Growth characteristics of representative C. elegans microbiota species

We obtained single colonies of CeMbio bacteria on TSA medium and observed their macroscopic features (**Fig. 1A**). At 25 °C, most species formed colonies by 24 h, except *Pseudomonas berkeleyensis* and *Sphingomonas molluscorum,* which required up to 48 h. Most bacteria formed circular, smooth, opaque, and smooth-edged colonies, with the exception of *Comamonas piscis*, which formed undulated colonies. In most cases, colonies were shades of yellow-beige, except for *Chryseobacterium scophthalmum* (orange) and *Enterobacter hormaechei* (white) (**Fig. 1A**); after three weeks at 4 °C, *C. scophthalmum* colonies turned dark brown and secreted a dark pigment that diffused throughout the medium. Microscopically, the CeMbio bacteria were Gram-negative bacilli, except for *C. piscis,* which were cocci or coccobacilli (**Fig. 1B**).

The CeMbio species also varied in their antibiotic susceptibility. We tested two concentrations each of ampicillin, erythromycin, kanamycin, and streptomycin (**Fig. S1A and Table 1**). For ampicillin, all the CeMbio bacteria were resistant at 50 µg ml^{-1}, and only *S. molluscorum* was susceptible to 50 µg ml^{-1}. For erythromycin, all the species were resistant at 10 µg ml^{-1}, except for *S. molluscorum* and *C. piscis.* At 50 µg ml^{-1}, only *E. hormaechei*, *S. indicatrix*, *Lelliottia amnigena*, and *P. lurida* were also resistant. For kanamycin, *Sphingobacterium multivorum*, *Stenotrophomonas indicatrix*, *C. scophthalmum*, and *Ochrobactrum vermis* were resistant to 50 µg ml^{-1}, while *P. lurida* was only resistant to 10 µg ml^{-1}. For streptomycin, *S. multivorum*, *S. indicatrix*, *C.*

scophthalmum, *S. molluscorum*, and *O. vermis* were resistant to 50 µg ml^{-1}, while *C. piscis*, *P. berkeleyensis*, and *P. lurida* were resistant only to 10 µg ml^{-1}. Thus, The CeMbio bacteria show extensive and partially overlapping antibiotic resistance. Three species (*O. vermis*, *S. multivorum,* and *C. scophthalmum*) exhibited resistance to all but 50 µg ml^{-1} erythromycin, and *S. indicatrix* was resistant to all. These results suggested that these *C. elegans*-associated bacteria are under strong selective pressure from antibiotics in the wild.

CeMbio bacteria differentially activate a PMK-1/p38-dependent gene reporter in the intestinal epithelium

The p38 MAPK pathway is the best understood host defense pathway in *C. elegans* (Kim *et al.*, 2002; Irazoqui *et al.*, 2010b). To better delineate its role during interactions with individual members of the microbiota, we measured the expression of a genetically-encoded fluorescent construct that is used to monitor its activity (Shivers *et al.*, 2010). This P*t24b8.5::gfp* reporter is induced in a *pmk-1*-dependent manner in the intestinal epithelium during intestinal infection by pathogens such as *P. aeruginosa* (Shivers *et al.*, 2009). Reference animals fed nonpathogenic *E. coli* on NGM media showed P*t24b8.5::gfp* expression in the anterior and posterior ends of the intestinal epithelium, with little basal expression in between (**Fig. 2A, E**). Animals fed *E. coli* on TSA showed increased P*t24b8.5::gfp* expression along the entire intestinal epithelium (**Fig. 2E, H**). Animals on TSA media alone, or infected with *S. aureus* on the same, showed decreased P*t24b8.5::gfp* expression relative to reference animals, ruling out a

158 nonspecific effect of the media and showing pathogen specificity of the reporter (**Fig.**
159 **2E, H**).

160 Animals that were mono-associated with distinct CeMbio bacteria showed differential
161 P*t24b8.5::gfp* expression. At one extreme, *Pantoea nemavictus* induced P*t24b8.5::gfp*
162 throughout the intestine, for an average ~2.5-fold compared with reference animals
163 (**Fig. 2C, F, and H**). At the other extreme, *C. scophthalmum* repressed P*t24b8.5::gfp*
164 about 2-fold (**Fig. 2D, G, and H**). The rest fell somewhere in between, with *L. amnigena,*
165 *P. berkeleyensis,* inducing P*t24b8.5::gfp* about 2-fold (high induction), *E. hormaechei,*
166 *A. guillouiae, S. molluscorum,* and *P. lurida* about 1.5-fold (modest induction), *S.*
167 *multivorum* and *S. indicatrix* about 1-fold (no induction), and *O. vermis* slightly
168 repressing (**Fig. 2F, G, and H**). These results suggested that the CeMbio bacteria may
169 vary in their activation of the PMK-1/p38 MAPK pathway and hinted that it may be
170 important for their interactions with *C. elegans*.

171

172 ***PMK-1 mediates host defense against distinct microbiota members***

173 To assess the role of PMK-1/p38 MAPK in interactions with CeMbio members, we
174 performed survival assays on individual species, comparing *pmk-1*-deficient animals to
175 wild type. First, we identified two informative times that enabled clear distinction of
176 bacteria that promoted or impaired survival, in both backgrounds. As references, the
177 median survival of wild type and *pmk-1(-)* animals exposed to nonpathogenic *E. coli* on
178 NGM medium was about 7 d; starved animals (no bacteria) on TSA medium showed

lifespan extension (median survival of 11 d); and *S. aureus*-infected animals showed decreased survival (medians of 2 and 1 d for wild type and *pmk-1(-),* respectively) (**Fig. 3A and B**). The differences among *S. multivorum*, *C. scophthalmum*, and *S. indicatrix* were best resolved at days 3 and 7, for both *C. elegans* genetic backgrounds (**Fig. 3A and B**). Thus, we chose these two time points for further study.

We measured survival after 3 and 7 days of exposure to the individual species of the CeMbio set, benchmarking against animals associated with nonpathogenic *E. coli*. For wild type animals, *P. nemavictus, L. amnigena, E. hormaechei, A. guillouiae, S. multivorum, S. indicatrix,* and *O. vermis* supported lifespan that was indistinguishable from control (**Fig. 3E and F**). We categorized these as "Neutral". *P. berkeleyensis, C. piscis, and C. scophthalmum* supported increased lifespan, while *P. lurida* and *S. molluscorum* shortened lifespan (**Fig. 3E and F**). We categorized these as "Probiotics" and "Pathogen", respectively. Thus, we identified *S. molluscorum* and *P. lurida* as CeMbio species that in mono-association may exhibit virulence towards wild type *C. elegans.* Consistent with this interpretation, *pmk-1* deletion further decreased survival on *P. lurida* (**Fig. 3D, F**), supporting the notion that PMK-1/p38 MAPK is important for host defense against virulence expressed by *P. lurida*.

Among the Probiotics, *pmk-1* deletion had no effect on host survival with *P. berkeleyensis,* showing that PMK-1/p38 MAPK is dispensable for lifespan extension by that bacterium. In contrast, *pmk-1* deletion reduced survival with *C. scophthalmum* and *C. piscis,* suggesting that PMK-1/p38 MAPK is important for lifespan promotion by those two species (**Fig. 3E, F**). Remarkably, *pmk-1(-)* mutants fared worse than wild type on

five of seven Neutrals, with the exceptions of *A. guillouiae* and *S. molluscorum* (**Fig. 3E, F**). Thus, PMK-1/p38 MAPK may play differential roles in maintaining or promoting lifespan (but not reducing it) when *C. elegans* is mono-associated with distinct members of its microbiota.

Taken together with the previous reporter expression data, these survival data defined four broad categories of CeMbio species (**Table 2**): Category 1, PMK-1 activated and required for defense (*P. nemavictus*, *P. lurida*, *C. piscis,* and *E. hormaechei*); Category 2, PMK-1 activated but not required for defense (*P. berkeleyensis*, *A. guillouiae*, *S. molluscorum* and *L. amnigena*); Category 3, PMK-1 not activated but required for defense (*S. multivorum* and *S. indicatrix*); and Category 4, PMK-1 repressed but required for survival (*O. vermis* and *C. scophthalmum*). These results demonstrate how activation of PMK-1/p38 MAPK signaling may not correlate well with its genetic requirement for protection against microbiota bacterial species.

CeMbio bacteria differentially activate an ACh-WNT gene reporter in the intestinal epithelium

To assess ACh-WNT signaling, we used a previously characterized genetically-encoded P*clec-60::gfp* fluorescent reporter. This reporter is rapidly induced in the intestinal epithelium in a pathogen- and ACh-WNT-dependent manner (Irazoqui *et al.*, 2010a). Reference animals on nonpathogenic *E. coli* showed low P*clec-60::gfp* expression and only in the posterior-most of intestinal ring, consistent with prior reports

(**Fig. 4A, E**). Also as reported, P*clec-60::gfp* expression extended anteriorly in animals infected with *S. aureus*, serving as positive control (Irazoqui *et al.*, 2010a; Labed *et al.*, 2018) (**Fig. 4B, E**). However, in contrast to previous reports where P*clec-60::gfp* was not induced by shorter starvation regimens (Labed *et al.*, 2018), by 24 h of starvation P*clec-60::gfp* expression did increase, providing an additional positive control **(Fig. 4H).**

As with P*t24b8.5::gfp,* P*clec-60::gfp* expression stratified the CeMbio bacteria in four broad categories. At one extreme, the "Activators" *A. guillouiae, S. multivorum,* and *C. scophthalmum* induced P*clec-60::gfp* expression anteriorly in the intestine, for an average of ≥ 2-fold compared to reference (**Fig. 4C, F, and H**). At the other extreme, the "Repressors" *P. berkeleyensis* and *P. lurida* repressed P*clec-60::gfp* expression about 1.5-fold (**Fig. 4D, G, and H**). The remaining bacteria fell in between. Aside from the "Non Inducers", *O. vermis* and *P. nemavictus* ("Modest Inducers") significantly but weakly induced P*clec-60::gfp* compared with controls (**Fig. 4F and H**). These results suggested that the ACh-WNT pathway may be differentially activated by distinct members of the CeMbio. However, because 24 h starvation also induced P*clec-60::gfp*, these results alone did not allow us to discriminate whether the inducer bacteria did so due to ACh-WNT pathway activation or due to poor nutrition. For this reason, and because not many bacteria activated *clec-60,* we chose to examine a third host defense pathway.

CeMbio bacteria differentially activate HLH-30/TFEB in the intestinal epithelium

To examine the activation of HLH-30/TFEB, we used a previously characterized construct that tags HLH-30 with GFP (HLH-30::GFP) (Visvikis *et al.*, 2014). In previous work we showed that HLH-30::GFP concentrates in cellular nuclei throughout the animal just 30 min after infection with *S. aureus* (Visvikis *et al.*, 2014). Reference animals on nonpathogenic *E. coli* showed little HLH-30::GFP nuclear localization, both in the intestine and the rest of the body (**Fig. 6A**). *S. aureus* induced strong nuclear localization throughout the entire body, serving as positive control (**Fig. 6B**). Remarkably, all of the CeMbio bacteria activated HLH-30::GFP in the intestinal epithelium (**Fig. 6E**). This activation could also be systemic, as most bacteria activated HLH-30::GFP also in the head (**Fig. 6F**), with the exceptions of *S. molluscorum* and *S. multivorum* (**Fig. 6C, F**). Thus, HLH-30/TFEB activation is a hallmark of mono-association with the CeMbio bacteria, suggesting that HLH-30/TFEB plays a fundamental role in interactions between *C. elegans* and its microbiota.

HLH-30/TFEB promotes host survival in interactions with distinct microbiota members

Following the same approach as for PMK-1/p38 MAPK, we used *hlh-30(-)* mutants to assess the role of HLH-30/TFEB in interactions with members of its CeMbio microbiota. The *E. coli*-associated references for both genotypes were indistinguishable at day 3 but could be resolved by day 7, as expected, given the known aging defect exhibited by *hlh-30*(-) animals (Visvikis *et al.*, 2014). The starved *hlh-30(-)* controls showed a dramatic loss of viability at day 7, consistent with previous reports (Settembre

et al., 2013).

At day 3, *hlh-30(-)* mutants fared equally well with *S. molluscorum, C. piscis* and *A. guillouiae,* as they did with *E. coli* (**Fig. 6A and C**). In contrast, the rest of the CeMbio bacteria reduced the survival of *hlh-30(-)* mutants relative to wild type at day 3, suggesting that HLH-30/TFEB is essential for host defense against these bacteria (**Fig. 6A and C**). At day 7, the relationships remained essentially the same, except for *C. piscis,* which caused earlier death of *hlh-30(-)* mutants compared to wild type (**Fig. 6B and D**). Thus, all the bacteria induced HLH-30/TFEB nuclear import and showed virulence towards *hlh-30*-deficient animals, except for *S. molluscorum* and *A. guillouiae,* which did not show virulence.

Acinetobacter guillouiae* promotes survival of infection with natural pathogen *Pseudomonas lurida

A. guillouiae activated all three pathways and did not exhibit virulence towards *pmk-1(-)* or *hlh-30(-)* animals, suggesting that it may possess probiotic properties. In contrast, *P. lurida* moderately induced PMK-1/p38 MAPK, strongly activated HLH-30/TFEB, and exhibited virulence towards wild type, *pmk-1(-),* and *hlh-30(-)* animals, suggesting that *P. lurida* possesses the hallmarks of an overt (and natural) pathogen of *C. elegans.*

Because PMK-1/p38 MAPK and HLH-30/TFEB are activated by *P. lurida* and both pathways are required for defense against its virulence, we tested if their prior activation

by *A. guillouiae* may be protective (**Fig. 7A**). A relatively short prior exposure of wild type animals to *A. guillouiae* significantly enhanced survival of *P. lurida* infection compared to *E. coli*-exposed controls (median survival ~5 days v. ~3 days, **Fig. 7B**), confirming that *A. guillouiae* protects *C. elegans* from *P. lurida* virulence.

A priori, A. guillouiae could protect *C. elegans* directly, by displacing *P. lurida* from the intestinal lumen (niche competition model) or indirectly, by inducing host defense (third-party competition model). To discriminate between these scenarios, we performed *A. guillouiae* protection assays with *pmk-1(-)* and *hlh-30(-)* mutants. Remarkably, deletion of either *pmk-1* (**Fig. 7C**) or *hlh-30* **(Fig. 7D**) completely suppressed the protection conferred by *A. guillouiae.* These results confirmed that protection conferred by *A. guillouiae* against *P. lurida* requires, and is likely mediated by, both the PMK-1/p38 MAPK and the HLH-30/TFEB pathways.

Recall that “nonpathogenic” *E. coli* activated PMK-1/p38 MAPK and HLH-30/TFEB on TSA medium (**Fig. 2H and 6G).** Prior exposure to *E. coli* on TSA medium also protected against *P. lurida* **(Sup Fig. 2A)**. *hlh-30* deletion animals showed protection towards *P. lurida* conferred by *E. coli* (**Sup Fig. 2B**). Thus, in this case HLH-30/TFEB pathway was not required for the probiotic effect of *E. coli.*

Discussion

We report here a phenotypic description of the reference *C. elegans* microbiota, known as CeMbio, including the morphological and growth characteristics of its members in vegetable-derived rich culture media in presence or absence of antibiotics, their ability to induce any of three important host defense pathways, and their ability to cause disease in animals that lack them. To our knowledge, this is the first systematic examination of these properties for every CeMbio member, at least under conditions that more closely resemble the natural niche of *C. elegans* than the standard nematode growth medium that is widely used in the laboratory.

The first key insight to emerge from these studies was that the ability of each bacterial species to induce reporters for a given host defense pathway did not correlate well with its virulence in wild type animals nor the requirement of that pathway for host defense against the bacteria (**Table 2, Fig. 8**). This is somewhat surprising, because a simple assumption might be that each host defense pathway evolved to detect and defend against bacteria that are virulent. We did find examples of bacteria that induced a reporter and were more virulent against animals that lacked the corresponding pathway, including some that showed “cryptic” virulence, or virulence that was masked by the (appropriate) host response. However, this was not the rule. What might be the evolutionary advantage to the host, or the inducing bacteria, to activate a host response if it does not protect the host against that infection? One possibility might be that the host response may protect the host against a second bacterial pathogen, enhancing the persistence and availability of the intestinal niche for the inducing bacteria.

A second key insight was that many CeMbio bacteria did not affect the survival of the host unless host defense was compromised (**Fig. 8**). In these examples, the bacteria would not be characterized as frank pathogens because they do not impair the survival of wild type animals compared to controls. Instead, they would fall under a category known as “opportunistic” pathogens, revealing that they do indeed possess pathogenic potential that is masked in immunocompetent animals, what we call ‘cryptic’ virulence (Casadevall and Pirofski, 2003; Casadevall and Pirofski, 2015). On the other hand, over-induction of a host response pathway could conceivably lead to disease, or improved health after removal of the pathway.

The third key insight was the host protection against *P. lurida,* the strongest frank pathogen in our dataset, by *A. guillouiae* (**Fig. 7B**). Both bacteria have been previously shown to persist in the *C. elegans* intestine (Pees *et al.*, 2021). Consistent with our finding that *P. lurida* exhibits virulence against *C. elegans,* the nematodes avoided *P. lurida* in food choice assays (Petersen *et al.*, 2021). However, under certain conditions *P. lurida* may also provide protection against infection, at least against pathogenic fungi (Dirksen *et al.*, 2016). *A priori,* protection against *P. lurida* pathogenesis by *A. guillouiae* could be mediated by colonization resistance (Sorbara and Pamer, 2019) or by immune-mediated protection (Kamada *et al.*, 2013). Our data show that disruption of either the PMK-1/p38 MAPK or the HLH-30/TFEB pathway abrogates such protection, supporting an immune-mediated antagonistic relationship – a ‘Third-Party’ model of microbe-microbe interaction. This result suggests that the order of colonization by these microbiota members may be a key determinant of host health under natural conditions. Further investigation is warranted to define the extent to which direct niche competition

may play a role as well. Moreover, it will be important to scale up this type of investigation into all potential microbe-microbe interaction pairs and, ultimately, entire communities *in vivo*.

Finally, our results clearly showed that HLH-30/TFEB becomes activated by ten out of twelve members of the CeMbio community. This observation suggests that HLH-30/TFEB is a key and broad element of microbiota-host interactions. It also suggests that there are commonalities among the ten activating species, which result in HLH-30/TFEB activation. It will be important to understand if these ten species are sensed by a common mechanism, or by distinct mechanisms that converge on HLH-30/TFEB. Future research should address the physiological consequences of HLH-30/TFEB activation on the host, on the bacteria, and on the community.

Acknowledgments

Thanks to the members of the IMP graduate program and of the Department of Microbiology and Physiological Systems for helpful discussions. The Sanderson Center for Optical Experimentation of the University of Massachusetts Chan Medical School provided microscopy support. Special gratitude to Dr. Amanda Wollenberg for initial work with microbiota isolates, and to Amy Parker, Annette Bohigian, Richard Fish, Tracey Rae, Marie Berardi, and Dhruti Desai for exceptional administrative support. Research reported in this publication was supported by the National Institute of General Medical Sciences of the National Institutes of Health under award numbers R01GM101056 and R35GM149284 (JEI), by the National Institute of Allergy and Infectious Diseases of the National Institutes of Health under award numbers T32AI095213 (XG), T32AI095213 (XG), and R21AI169842 (JEI), and by the Dr. Marcellette G. Williams Memorial Fund (JEI). Some strains were provided by the CGC, which is funded by NIH Office of Research Infrastructure Programs (P40OD010440). The content is solely the responsibility of the authors and does not necessarily represent the official views of the National Institutes of Health.

Experimental Procedures

Strains, media, and culture conditions

C. elegans strains were maintained on nematode-growth media (NGM) plates seeded with *E. coli* OP50 at 15 – 20°C, according to standard procedures (Powell and Ausubel, 2008). See **Table 4** for strain genotype details. The *C. elegans* microbiota kit was purchased through the Caenorhabditis Genetics Center (CGC).

CeMbio cultures were grown under aerobic conditions at 25 °C with 170-200 RPM shaking in TSB (Sigma-Aldrich T8907) containing 50 µg ml^{-1} ampicillin for 20-24 h. 10 µL of the CeMbio culture was then spread on TSA (BD 236950) containing 50 µg ml^{-1} ampicillin plates for 20-24 h at 25 °C. TSA containing 50 µg ml^{-1} ampicillin plates were made within 10 days of use for experiments. Tryptic soy agar (TSA), as a plant hydrolysate, is a closer approximation to the natural environment from which they were isolated than other more traditional media (e.g., NGM or Luria-Bertani) (Stiernagle, 2006).

S. aureus SH1000 was grown overnight in TSB containing 50 µg ml^{-1} kanamycin, 37 °C at 200 RPM. 10 µL of overnight cultures was spread on the surface of 35 mm TSA containing 10 µg ml^{-1} kanamycin and incubated 5–6 h at 37 °C. Animals were transferred to each of three replicate infection plates. Survival was quantified as described (Powell and Ausubel, 2008).

For *E. coli* OP50 grown on TSA plates, *E. coli* was grown overnight in LB (MP Biomedicals 113002032) containing 100 µg ml^{-1} streptomycin, 37 °C at 170-200 RPM.

10 µL of overnight culture was spread on the surface of 35 mm TSA containing 50 µg ml^{-1} ampicillin, and incubated 25 °C, similarly to CeMbio. Control NGM plates were seeded with 200 µL of overnight culture and incubated at 25 °C.

Survival

For *hlh-30* and *pmk-1* mutant animals: Animals were staged by transferring egg laying adults to *E. coli* NGM plates and allowed to lay eggs for 2-3 hours. Egg laying adults were then removed. Progeny were placed at 15 °C overnight and then shifted to 20 °C for 2 days, reaching L4/Young adult (YA) stage. YA animals were washed 10x in 10-14mL 1xM9 buffer and transferred to UV-arrested E. coli (UV-arrested to minimize carry over of E. coli in subsequent steps). YA animals on UV-*E. coli* were grown at 25C overnight (*spe-9*(hc88) I ; *rrf-3*(b26) II mutants are fertilization defective at 25°C. The adult animals are then transferred onto full lawn plates of *S. aureus*, *E. coli*, starvation, and CeMbio plates, 3-2 technical replicates per genotype.

A. guillouiae protection

L4 animals were placed at 25 °C for 20-24 h to reach YA stage. ~100 YA animals were then placed on *E. coli* NGM/TSA plates or A. *guillouiae* for 8 h at 25 °C. After 8 h, ~30 animals were transferred on *P. lurida* plates in triplicate, placed at 25 °C, and scored every day.

418

419 *Image acquisition and analysis*

420 Images were taken using a Lionheart FX automatic microscope (BioTek
421 Instruments) using 4x objective. 10-25 YA animals were placed onto bacterial plates
422 and imaged after 30 min for HLH-30::GFP, 4 h for P*fmo-2::gfp*, 24 h for P*t24b8.5::gfp*
423 and P*clec-60::gfp* at 25 °C. Fluorescence microscopy experiments were repeated total
424 of 3 independent times. Animals were anesthetized using 100 mM NaN_3 (Sigma-Aldrich
425 S2002) on a 4% agar pad for imaging. All images were captured at the same exposure
426 and intensity in a biological replicate. Greyscale images were used for image analysis.
427 FIJI was used for image analysis. A region of interest (ROI) was drawn using
428 segmented line tool along the intestine or whole animal, from anterior to posterior.

429 For P*t24b8.5::gfp*, and P*clec-60::gfp*, mean fluorescent intensity (MFI) of the ROI,
430 anterior to posterior intestine, was determined by using the Analyze>Multi Plot function.
431 Pixel length was transformed to percent length in excel, each percent length value has a
432 single value. All percent length-MFI values were rounded up to the nearest whole
433 percent length number in excel. Area under the curve was calculated using GraphPad
434 PRISM9 and normalized to *E. coli* control.

435 For HLH-30::GFP animals, an ROI of the head (from mouth to pharyngeal bulb) and
436 the anterior half of intestine was acquired. A threshold was applied to images by
437 converting RAW grayscale image to 8bit. The threshold was determined by the most
438 HLH-30::GFP nuclei on *S. aureus* and least HLH-30::GFP nuclei on *E. coli* treated

439 animals. The threshold is the same within a biological replicate. ROI's were selected
440 using ROI Manager>"OR (Combine)" and analyzed using Analyze Particles. Analyze
441 Particles set values are Size=1-20, Circularity=0-1.

442 For single colony pictures, bacteria were streaked out on TSA + 50 µg ml^{-1} Ampicillin
443 plates and placed at 25 °C until colonies were seen, 24 – 48 h. Pictures were taken
444 once single colonies were visible using iPhone 11 camera through dissecting
445 microscope eyepieces on 3.5x zoom.

446 For antibiotic resistance, ampicillin, erythromycin, kanamycin, and streptomycin were
447 used. The antibiotics was added once autoclaved TSA media cooled and then added to
448 single well plates. CeMbio was grown in TSB at 25C for 24 h, and 2 µL of culture was
449 pipetted onto the TSA + antibiotic plates. CeMbio were placed at 25 °C for 24 h and
450 picture was taken using iPhone 11 camera.

451 *Statistics*

452 Statistics analyses were performed in GraphPad PRISM9. For comparison of
453 survival curves, a Log-rank (Mantel-Cox) test was performed. For % survival on CeMbio
454 at days 3 and 7, an ordinary two-way ANOVA, Dunnett's multiple comparisons test was
455 performed. For fluorescence analyses, an ordinary one-way ANOVA, Dunnett's multiple
456 comparisons test, compared to *E. coli* controls was performed. A p-value ≤ 0.05 was
457 considered significantly different from control.

References

Berg, M., Monnin, D., Cho, J., Nelson, L., Crits-Christoph, A., and Shapira, M. (2019) TGFβ/BMP immune signaling affects abundance and function of C. elegans gut commensals. *Nat Commun* **10**: 604.

Berg, M., Stenuit, B., Ho, J., Wang, A., Parke, C., Knight, M., *et al.* (2016) Assembly of the Caenorhabditis elegans gut microbiota from diverse soil microbial environments. *ISME J* **10**: 1998–2009.

Brand, M.W., Wannemuehler, M.J., Phillips, G.J., Proctor, A., Overstreet, A.-M., Jergens, A.E., *et al.* (2015) The Altered Schaedler Flora: Continued Applications of a Defined Murine Microbial Community. *ILAR J* **56**: 169–178.

Caballero-Flores, G., Pickard, J.M., and Núñez, G. (2023) Microbiota-mediated colonization resistance: mechanisms and regulation. *Nat Rev Microbiol* **21**: 347–360.

Casadevall, A., and Pirofski, L. (2003) The damage-response framework of microbial pathogenesis. *Nat Rev Microbiol* **1**: 17–24.

Casadevall, A., and Pirofski, L. (2015) What Is a Host? Incorporating the Microbiota into the Damage-Response Framework. *Infect Immun* **83**: 2–7.

Dirksen, P., Assié, A., Zimmermann, J., Zhang, F., Tietje, A.-M., Marsh, S.A., *et al.* (2020) CeMbio - The Caenorhabditis elegans Microbiome Resource. *G3 Genes Genomes Genetics* **10**: g3.401309.2020.

Dirksen, P., Marsh, S.A., Braker, I., Heitland, N., Wagner, S., Nakad, R., *et al.* (2016) The native microbiome of the nematode Caenorhabditis elegans: gateway to a new host-microbiome model. *Bmc Biol* **14**: 38.

Eberl, G. (2010) A new vision of immunity: homeostasis of the superorganism. *Mucosal Immunol* **3**: 450–460.

Fletcher, M., Tillman, E.J., Butty, V.L., Levine, S.S., and Kim, D.H. (2019) Global transcriptional regulation of innate immunity by ATF-7 in C. elegans. *PLoS Genet* **15**: e1007830.

Gasaly, N., Vos, P. de, and Hermoso, M.A. (2021) Impact of Bacterial Metabolites on Gut Barrier Function and Host Immunity: A Focus on Bacterial Metabolism and Its Relevance for Intestinal Inflammation. *Front Immunol* **12**: 658354.

Geva-Zatorsky, N., Sefik, E., Kua, L., Pasman, L., Tan, T.G., Ortiz-Lopez, A., *et al.* (2017) Mining the Human Gut Microbiota for Immunomodulatory Organisms. *Cell* **168**: 928-943.e11.

Harding, B.W., and Ewbank, J.J. (2021) An integrated view of innate immune mechanisms in C. elegans. *Biochem Soc Trans* **49**: 2307–2317.

Horrocks, V., King, O.G., Yip, A.Y.G., Marques, I.M., and McDonald, J.A.K. (2023) Role of the gut microbiota in nutrient competition and protection against intestinal pathogen colonization. *Microbiology* **169**: 001377.

Huttenhower, C., Gevers, D., Knight, R., Abubucker, S., Badger, J.H., Chinwalla, A.T., *et al.* (2012) Structure, function and diversity of the healthy human microbiome. *Nature* **486**: 207–214.

Irazoqui, J.E., Troemel, E.R., Feinbaum, R.L., Luhachack, L.G., Cezairliyan, B.O., and Ausubel, F.M. (2010a) Distinct Pathogenesis and Host Responses during Infection of C. elegans by P. aeruginosa and S. aureus. *Plos Pathog* **6**: e1000982.

Irazoqui, J.E., Urbach, J.M., and Ausubel, F.M. (2010b) Evolution of host innate defence: insights from Caenorhabditis elegans and primitive invertebrates. *Nat Rev Immunol* **10**: 47–58.

Kamada, N., Seo, S.-U., Chen, G.Y., and Núñez, G. (2013) Role of the gut microbiota in immunity and inflammatory disease. *Nat Rev Immunol* **13**: 321–335.

Kim, D.H., Feinbaum, R., Alloing, G., Emerson, F.E., Garsin, D.A., Inoue, H., *et al.* (2002) A Conserved p38 MAP Kinase Pathway in Caenorhabditis elegans Innate Immunity. *Science* **297**: 623–626.

Kostic, A.D., Howitt, M.R., and Garrett, W.S. (2013) Exploring host–microbiota interactions in animal models and humans. *Genes Dev* **27**: 701–718.

Labed, S.A., Wani, K.A., Jagadeesan, S., Hakkim, A., Najibi, M., and Irazoqui, J.E. (2018) Intestinal Epithelial Wnt Signaling Mediates Acetylcholine-Triggered Host Defense against Infection. *Immunity* **48**: 963-978.e3.

Lawley, T.D., Clare, S., Walker, A.W., Stares, M.D., Connor, T.R., Raisen, C., *et al.* (2012) Targeted Restoration of the Intestinal Microbiota with a Simple, Defined Bacteriotherapy Resolves Relapsing Clostridium difficile Disease in Mice. *PLoS Pathog* **8**: e1002995.

Marinos, G., Hamerich, I.K., Debray, R., Obeng, N., Petersen, C., Taubenheim, J., *et al.* (2023) Metabolic model predictions enable targeted microbiome manipulation through precision prebiotics. *bioRxiv* 2023.02.17.528811.

Marples, R.R., and Kligman, A.M. (1971) Ecological Effects of Oral Antibiotics on the Microflora of Human Skin. *Arch Dermatol* **103**: 148–153.

Marples, R.R., Kligman, A.M., Lantis, L.R., and Downing, D.T. (1970) The Role of the Aerobic Microflora in the Genesis of Fatty Acids in Human Surface Lipids* * From the Department of Dermatology, School of Medicine, University of Pennsylvania, Philadelphia, Pennsylvania 19104 and the Departments of Dermatology and Biochemistry, Boston University School of Medicine, Boston. Massachusetts 02118.‡. *J Investig Dermatol* **55**: 173–178.

Obeng, N., Czerwinski, A., Schütz, D., Michels, J., Leipert, J., Bansept, F., *et al.* (2023) Bacterial c-di-GMP has a key role in establishing host–microbe symbiosis. *Nat Microbiol* **8**: 1809–1819.

Ortiz, A., Vega, N.M., Ratzke, C., and Gore, J. (2021) Interspecies bacterial competition regulates community assembly in the C. elegans intestine. *Isme J* 1–15.

Pees, B., Johnke, J., Möhl, M., Hamerich, I.K., Leippe, M., and Petersen, C. (2021) Microbes to□go: Slugs as source for C. elegans microbiota acquisition. *Environ Microbiol* .

Peixoto, R.S., Harkins, D.M., and Nelson, K.E. (2020) Advances in Microbiome Research for Animal Health. *Annu Rev Anim Biosci* **9**: 1–23.

Petersen, C., Pees, B., Christophersen, C.M., and Leippe, M. (2021) Preconditioning With Natural Microbiota Strain Ochrobactrum vermis MYb71 Influences Caenorhabditis elegans Behavior. *Front Cell Infect Mi* **11**: 775634.

Powell, J.R., and Ausubel, F.M. (2008) Innate Immunity. *Methods Mol Biol (Clifton, NJ)* **415**: 403–427.

Rogala, A.R., Oka, A., and Sartor, R.B. (2020) Strategies to Dissect Host-Microbial Immune Interactions That Determine Mucosal Homeostasis vs. Intestinal Inflammation in Gnotobiotic Mice. *Front Immunol* **11**: 214.

Settembre, C., Cegli, R.D., Mansueto, G., Saha, P.K., Vetrini, F., Visvikis, O., *et al.* (2013) TFEB controls cellular lipid metabolism through a starvation-induced autoregulatory loop. *Nat Cell Biol* **15**: 647–658.

Shilov, V.M., Lizko, N.N., Borisova, O.K., and Prokhorov, V.Y. (1971) Changes in the microflora of man during long-term confinement. *Life Sci space Res* **9**: 43–9.

Shivers, R.P., Kooistra, T., Chu, S.W., Pagano, D.J., and Kim, D.H. (2009) Tissue-Specific Activities of an Immune Signaling Module Regulate Physiological Responses to Pathogenic and Nutritional Bacteria in C. elegans. *Cell Host Microbe* **6**: 321–330.

Shivers, R.P., Pagano, D.J., Kooistra, T., Richardson, C.E., Reddy, K.C., Whitney, J.K., *et al.* (2010) Phosphorylation of the Conserved Transcription Factor ATF-7 by PMK-1 p38 MAPK Regulates Innate Immunity in Caenorhabditis elegans. *PLoS Genet* **6**: e1000892.

Sorbara, M.T., and Pamer, E.G. (2019) Interbacterial mechanisms of colonization resistance and the strategies pathogens use to overcome them. *Mucosal Immunol* **12**: 1–9.

Stiernagle, T. (2006) Maintenance of C. elegans. *WormBook* 1–11.

Taylor, M., and Vega, N.M. (2021) Host Immunity Alters Community Ecology and Stability of the Microbiome in a Caenorhabditis elegans Model. *Msystems* **6**.

Visvikis, O., Ihuegbu, N., Labed, S.A., Luhachack, L.G., Alves, A.-M.F., Wollenberg, A.C., *et al*. (2014) Innate Host Defense Requires TFEB-Mediated Transcription of Cytoprotective and Antimicrobial Genes. *Immunity* **40**: 896–909.

Wang, B., Yao, M., Lv, L., Ling, Z., and Li, L. (2017) The Human Microbiota in Health and Disease. *Engineering* **3**: 71–82.

Weitekamp, C.A., Kvasnicka, A., Keely, S.P., Brinkman, N.E., Howey, X.M., Gaballah, S., *et al*. (2021) Monoassociation with bacterial isolates reveals the role of colonization, community complexity and abundance on locomotor behavior in larval zebrafish. *Anim Microbiome* **3**: 12.

Figure legends

Figure 1. Growth and morphological characteristics of CeMbio bacteria.

A. Representative images of individual CeMbio colonies grown on TSA at 25 °C for 24-48 h. Scale bars = 1 mm.

B. Gram staining of individual CeMbio cultures grown overnight in TSB at 25 °C for 24 h. Scale bars = 5 µm.

Figure 2. *C. elegans* microbiota bacteria differentially activate P*t24b8.5::gfp* expression along the intestinal epithelium.

A - D. Representative brightfield and epifluorescence micrographs of P*t24b8.5::gfp* animals fed *E. coli*, *S. aureus*, *P. nemavictus*, and *C. scophthalmum* for 24 h at 25 °C. Animals were straightened using FIJI. Scale bars = 200 µm.

E - G. P*t24b8.5::gfp* mean fluorescent intensity (MFI) along the intestine of animals exposed to the indicated bacteria for 24 h at 25 °C. Representative of 3 biological replicates, n = 15 - 25 animals per biological replicate.

H. Area under the curve (AUC) quantitative analysis of P*t24b8.5::gfp* expression in the intestine, normalized to *E. coli* control. Animals fed on the indicated bacteria for 24 h at 25 °C. Three biological replicates, n = 15 – 25 animals per biological replicate. ****$p \leq 0.0001$; *$p \leq 0.05$, ordinary one-way ANOVA, Dunnett's multiple comparisons test, compared to *E. coli* controls.

Figure 3. PMK-1/p38 MAPK is differentially required for *C. elegans* survival on distinct CeMbio bacteria.

A and B. Survival of wild type (A) or *pmk-1(km25)* (B) animals after transfer to full lawns of CeMbio bacterial monoculture on TSA at 25 °C with the indicated antibiotics to prevent *E. coli* contamination. Data are representative of two biological replicates. Error bars are ± SEM. n = 50 - 100 animals per condition per replicate.

C – F. Survival of wild type and *pmk-1(km25)* animals after transfer to full lawns of CeMbio bacterial monoculture on TSA at 25 °C on days 3 (C and D) and 7 (E and F). Trials were performed in two internally controlled batches as shown. Data points represent median survival from individual biological replicates; at least 2 biological replicates for each treatment. Error bars are ± SEM. n = 50 - 100 animals per condition per replicate. ****$p \leq 0.0001$, ***$p \leq 0.001$, **$p \leq 0.01$, *$p \leq 0.05$, ordinary two-way ANOVA, Dunnett's multiple comparisons test.

Figure 4. *C. elegans* microbiota bacteria differentially activate P*clec-60::gfp* expression along the intestinal epithelium.

A - D. Representative brightfield and epifluorescence micrographs of P*clec-60::gfp* animals fed *E. coli*, *S. aureus*, *L. amnigena*, and *C. scophthalmum* for 24 h at 25 °C. Scale bars = 200 µm.

608 **E - G.** P*clec-60::gfp* mean fluorescent intensity (MFI) along the intestine of animals
609 exposed to the indicated bacteria for 24 h at 25 °C. Representative of 3 biological
610 replicates, n = 15 - 25 animals per biological replicate.

611 **H.** Area under the curve (AUC) quantitative analysis of P*clec-60::gfp* expression in the
612 intestine, normalized to *E. coli* control. Animals fed on the indicated bacteria for 24 h at
613 25 °C. Three biological replicates, n = 15 – 25 animals per biological replicate. ****$p \leq$
614 0.0001, ***$p \leq 0.001$, **$p \leq 0.01$, *$p \leq 0.05$, ordinary one-way ANOVA, Dunnett's multiple
615 comparisons test, compared to *E. coli* controls.

616

617 **Figure 5. *C. elegans* microbiota bacteria differentially drive HLH-30::GFP nuclear**
618 **localization.**

619 **A - D.** Representative brightfield and epifluorescence micrographs of P*hlh-30::hlh-*
620 *30a::gfp* (HLH-30::GFP) animals fed *E. coli*, *S. aureus, S. molluscorum*, and *C.*
621 *scophthalmum* for 30 min at 25 °C. Scale bars = 200 µm.

622 E and F) Representative epifluorescence micrographs of HLH-30::GFP animals
623 posterior intestine fed *E. coli* or *S. aureus* for 30 min at 25 °C. Scale bars = 50 µm

624 H and I) Representative epifluorescence micrographs of HLH-30::GFP animals head fed
625 *E. coli* or *S. aureus* for 30 min at 25 °C. Scale bars = 20 µm

626

627 **G and H.** Quantitative analysis of HLH-30::GFP nuclear localization in the intestinal

epithelium (G) or head (H) of animals fed the indicated bacteria for 30 min. Data are means ± SEM for three biological replicates; n = 15 - 25 animals per biological replicate. ****$p \leq 0.0001$, ***$p \leq 0.001$, **$p \leq 0.01$, *$p \leq 0.05$, ordinary one-way ANOVA, Dunnett's multiple comparisons test, compared to *E. coli* controls.

Figure 6. HLH-30 is differentially required for *C. elegans* survival on distinct CeMbio bacteria.

A – D. Survival of wild type and *hlh-30(tm1978)* animals after transfer to full lawns of CeMbio bacterial monoculture on TSA at 25 °C on days 3 (A and B) and 7 (C and D). Trials were performed in two internally controlled batches as shown. Data points represent median survival from individual biological replicates; at least 2 biological replicates for each treatment. Error bars are ± SEM. n = 50 - 100 animals per condition per replicate. ****$p \leq 0.0001$, ***$p \leq 0.001$, **$p \leq 0.01$, *$p \leq 0.05$, ordinary two-way ANOVA, Dunnett's multiple comparisons test.

Figure 7. *A. guillouiae* exerts immune-mediated host protection against *P. lurida* infection.

A. Schematic of the experimental approach. Animals were transferred from *E. coli* to *A. guillouiae* on TSA for 8 h at 25 °C. Subsequently, they were transferred to full lawns of *P. lurida* on TSA at 25 °C and scored for survival. In parallel, controls animals were transferred to *E. coli* instead of *A. guillouiae* and treated identically.

649 **B.** Survival of *P. lurida* infection of wild type animals pre-exposed to *E. coli* or *A.*
650 *guillouiae* for 8 h. Representative of 3 biological replicates, n = 50-100 animals. Error
651 bars are ± SEM from 3 technical replicates. ****$p \leq 0.0001$, ***$p \leq 0.001$, **$p \leq 0.01$, *$p \leq$
652 0.05, Kaplan-Meier Log-rank (Mantel-Cox) test.

653 **C.** Survival of *P. lurida* infection of pre-exposed wild type and *pmk-1(-)* animals.
654 Representative of 3 biological replicates, n = 50-100 animals. Error bars are ± SEM
655 from 3 technical replicates. ****$p \leq 0.0001$, ***$p \leq 0.001$, **$p \leq 0.01$, *$p \leq 0.05$, Kaplan-
656 Meier Log-rank (Mantel-Cox) test.

657 **D.** Survival of *P. lurida* infection of pre-exposed wild type and *hlh-30(-)* animals.
658 Representative of 3 biological replicates, n = 50-100 animals. Error bars are SEM from
659 3 technical replicates. ****$p \leq 0.0001$, ***$p \leq 0.001$, **$p \leq 0.01$, *$p \leq 0.05$, Kaplan-Meier
660 Log-rank (Mantel-Cox) test.

661

662 **Figure 8. Summary of pathway analysis data.**

663 Reporter activity and survival at days 3 and 7 of animals exposed to the indicated
664 CeMbio bacteria. Represented data are from Fig. 2 - 6. In the survival heat maps, the
665 WT data are represented twice to facilitate comparison with the *pmk-1(-)* and *hlh-30(-)*
666 mutants.

667

668 **Supplemental Figure 1. Antibiotic resistance of CeMbio bacteria.**

669 Growth on TSA with indicated antibiotics of 2 µl overnight aliquots for 24 h at 25 °C.

670

671 **Supplemental Figure 2. *E. coli* on TSA protects against *P. lurida*.**

672 **A.** Survival of *P. lurida* infection of wild type animals pre-exposed to *E. coli* on NGM or
673 TSA for 8 h. Representative of 2 biological replicates, n = 50-100 animals. Error bars
674 are ± SEM from 3 technical replicates. $^{**}p \leq 0.01$, $^{*}p \leq 0.05$, Kaplan-Meier Log-rank
675 (Mantel-Cox) test.

676 **B.** Survival of *P. lurida* infection of *hlh-30(-)* deficient animals pre-exposed to *E. coli* on
677 NGM or TSA for 8 h. Representative of 2 biological replicates, n = 50-100 animals. Error
678 bars are ± SEM from 3 technical replicates. $^{*}p \leq 0.05$, Kaplan-Meier Log-rank (Mantel-
679 Cox) test.

680

681 **Table 1. Antibiotic susceptibility of the 12 CeMbio isolates**

682 **Table 2. Categorization of CeMbio isolates according to reporter expression and**
683 **effect of PMK-1 deletion on survival**

684 **Table 3. Categorization of CeMbio isolates according to reporter expression and**
685 **effect of HLH-30 deletion on survival**

686 **Table 4. *C. elegans* strains used**

687

Gonzalez et al Figure 1

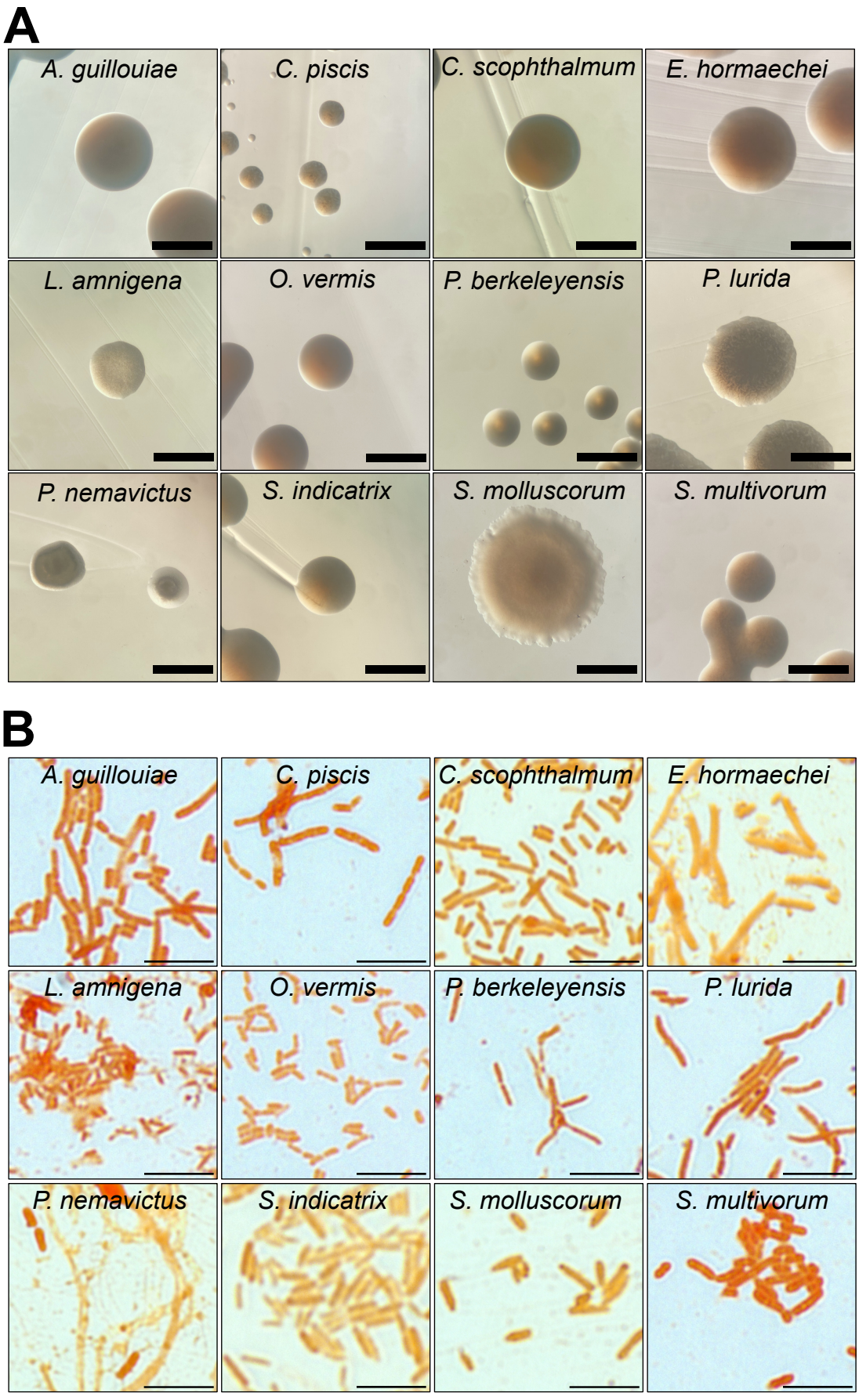

Gonzalez et al Figure 2

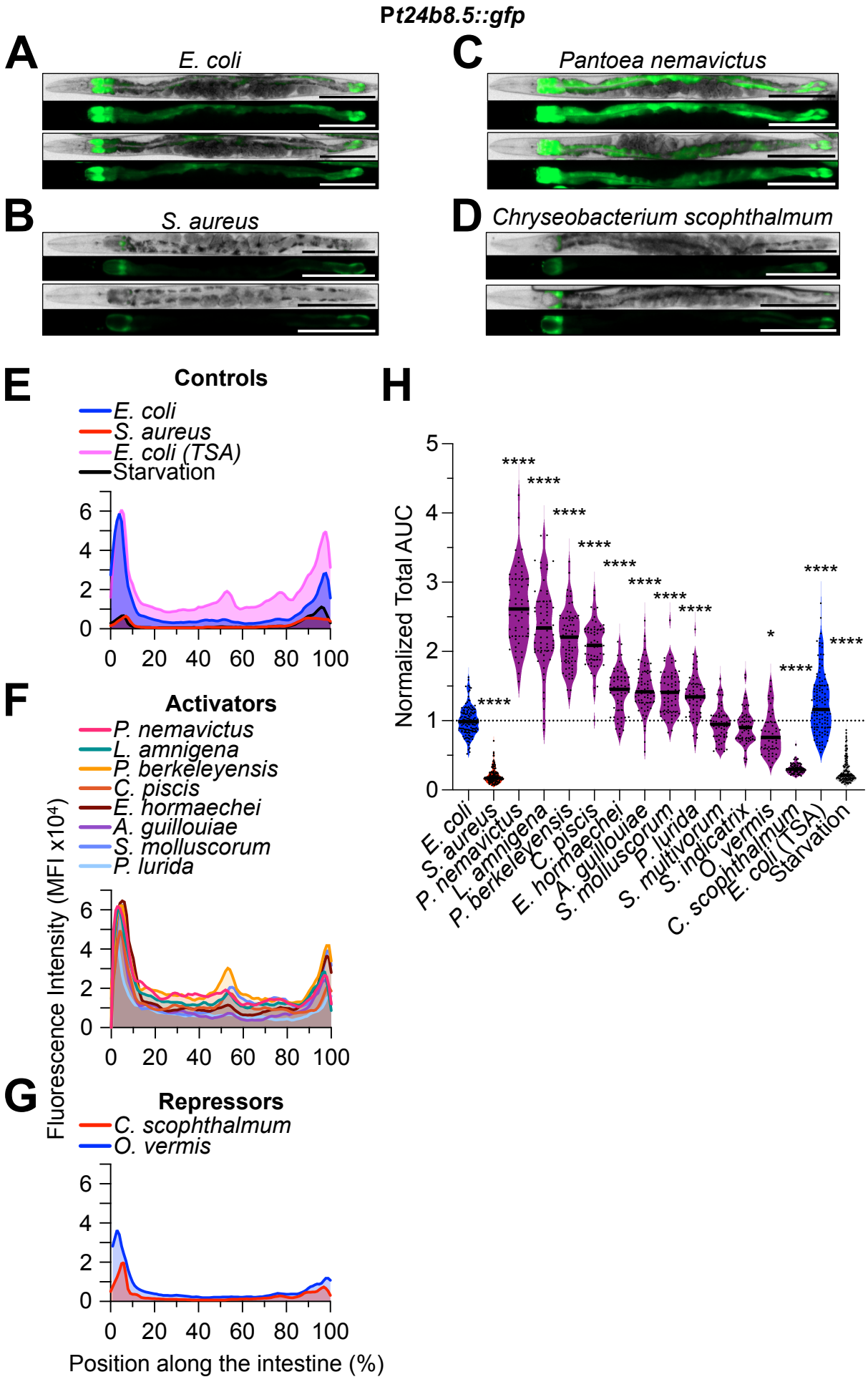

Gonzalez et al Figure 3

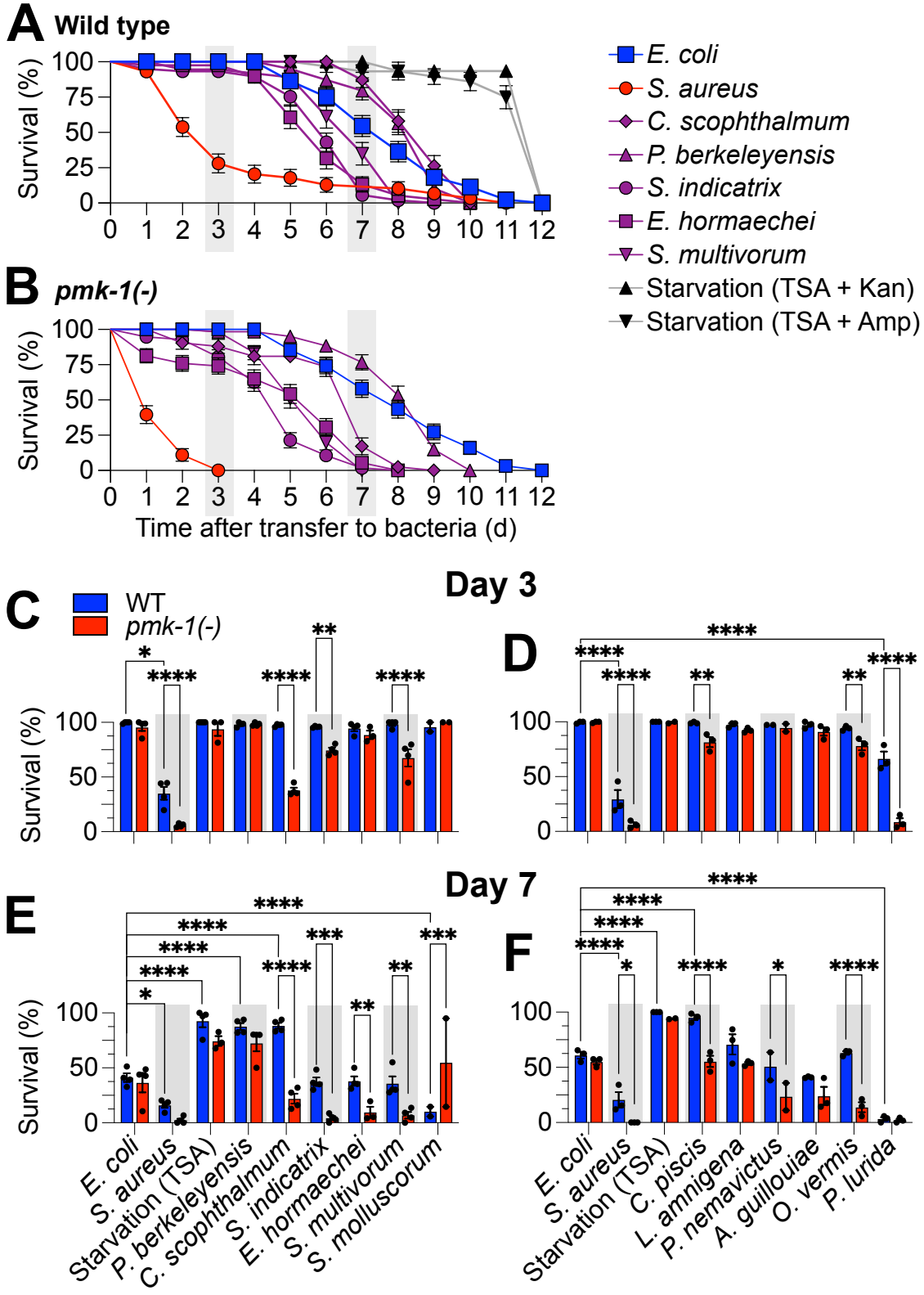

Gonzalez et al Figure 4

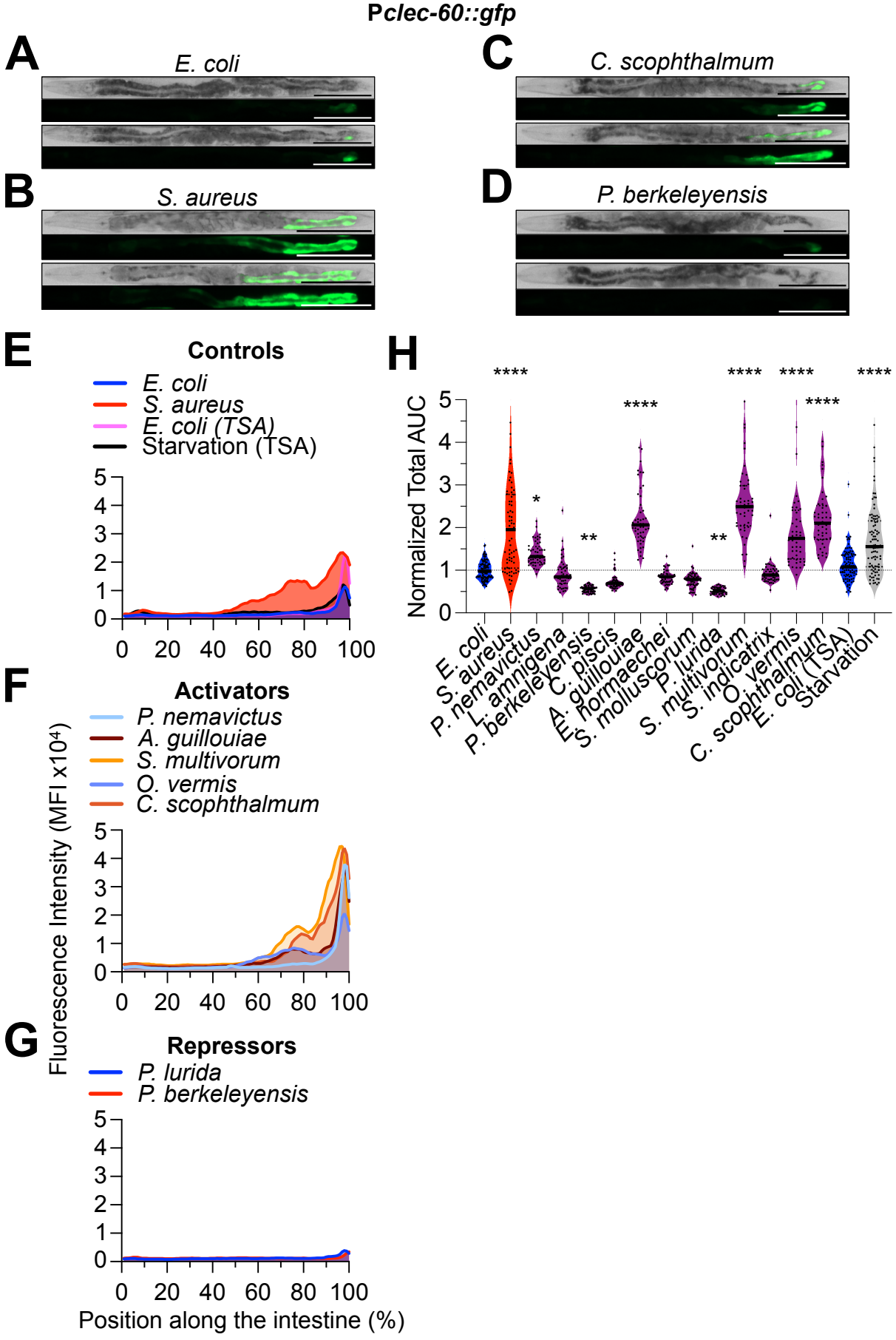

Gonzalez et al Figure 5

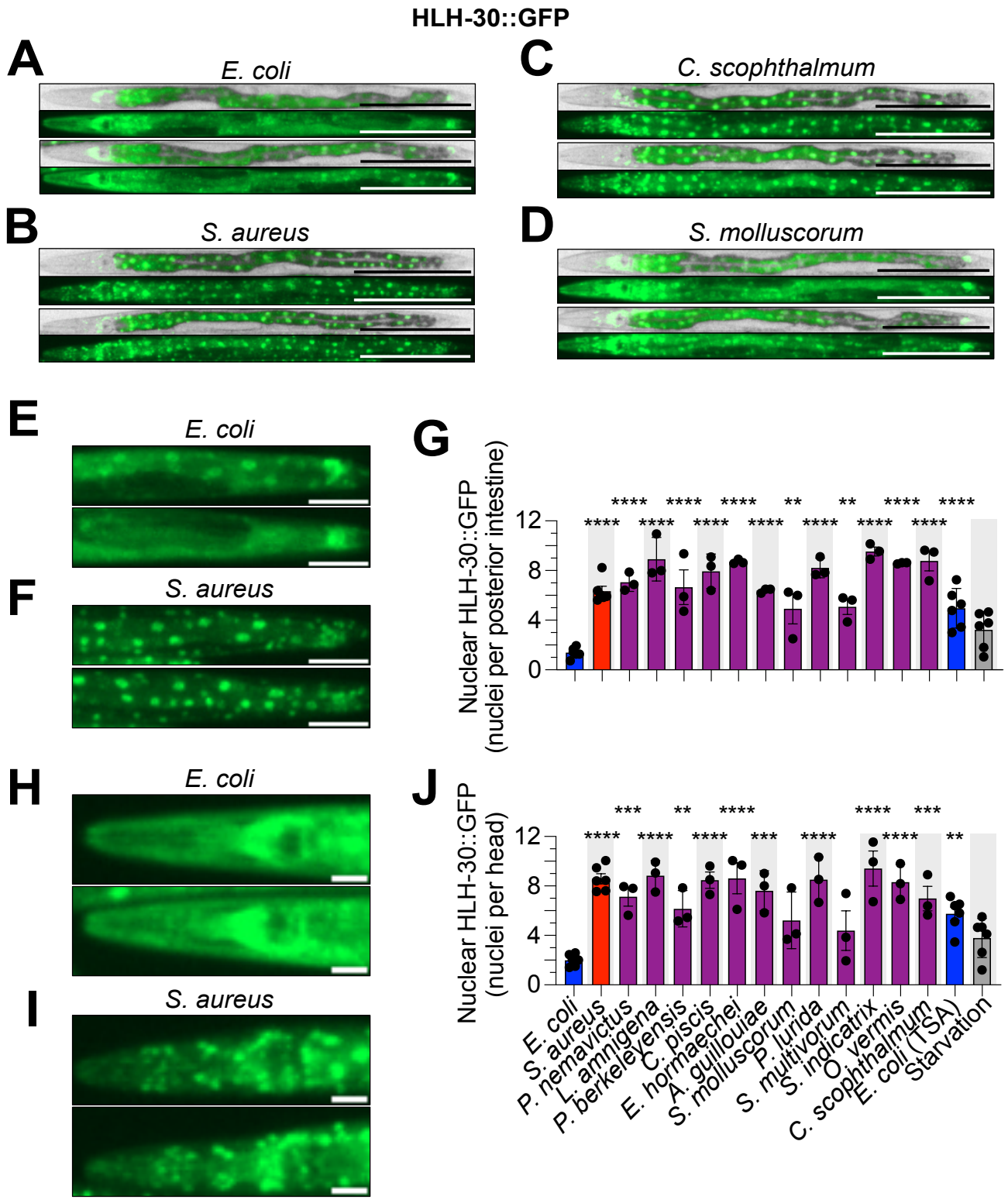

Gonzalez et al Figure 6

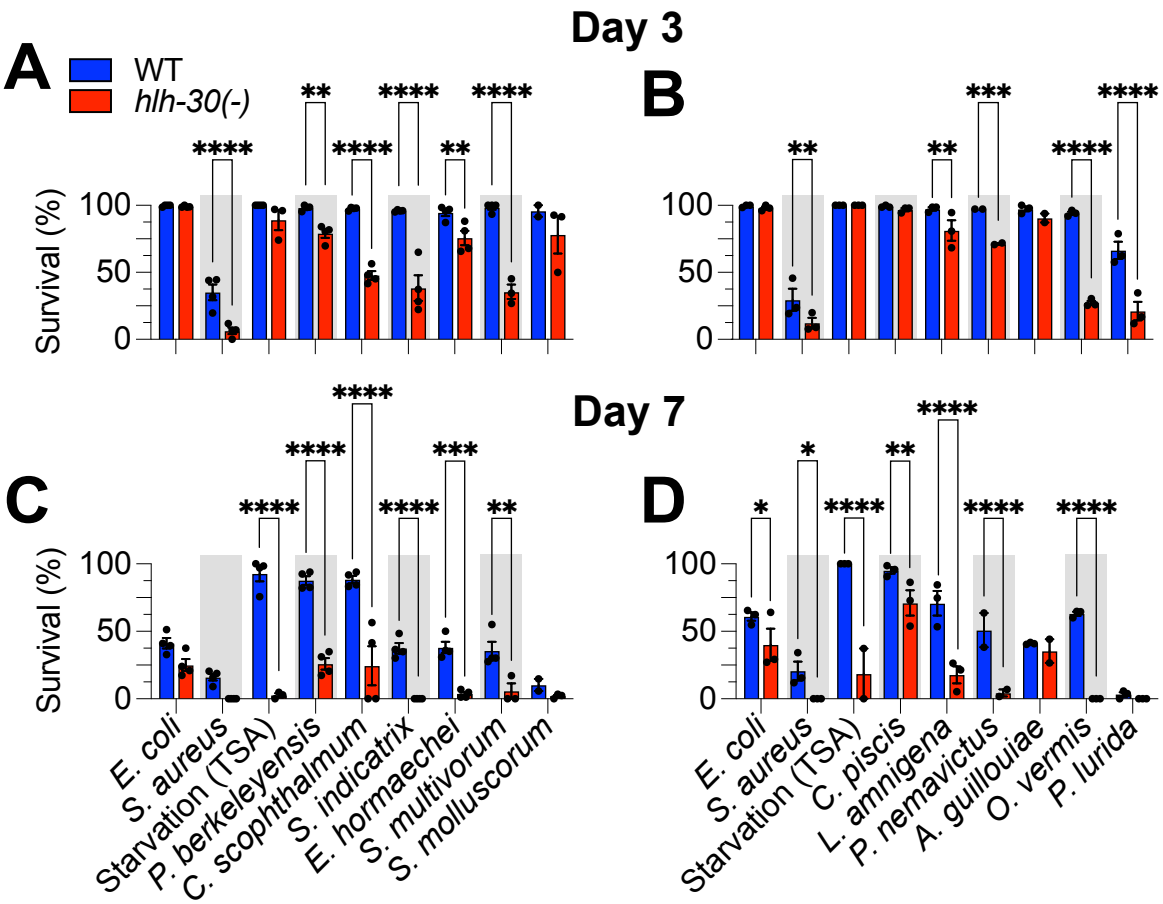

González et al Figure 7

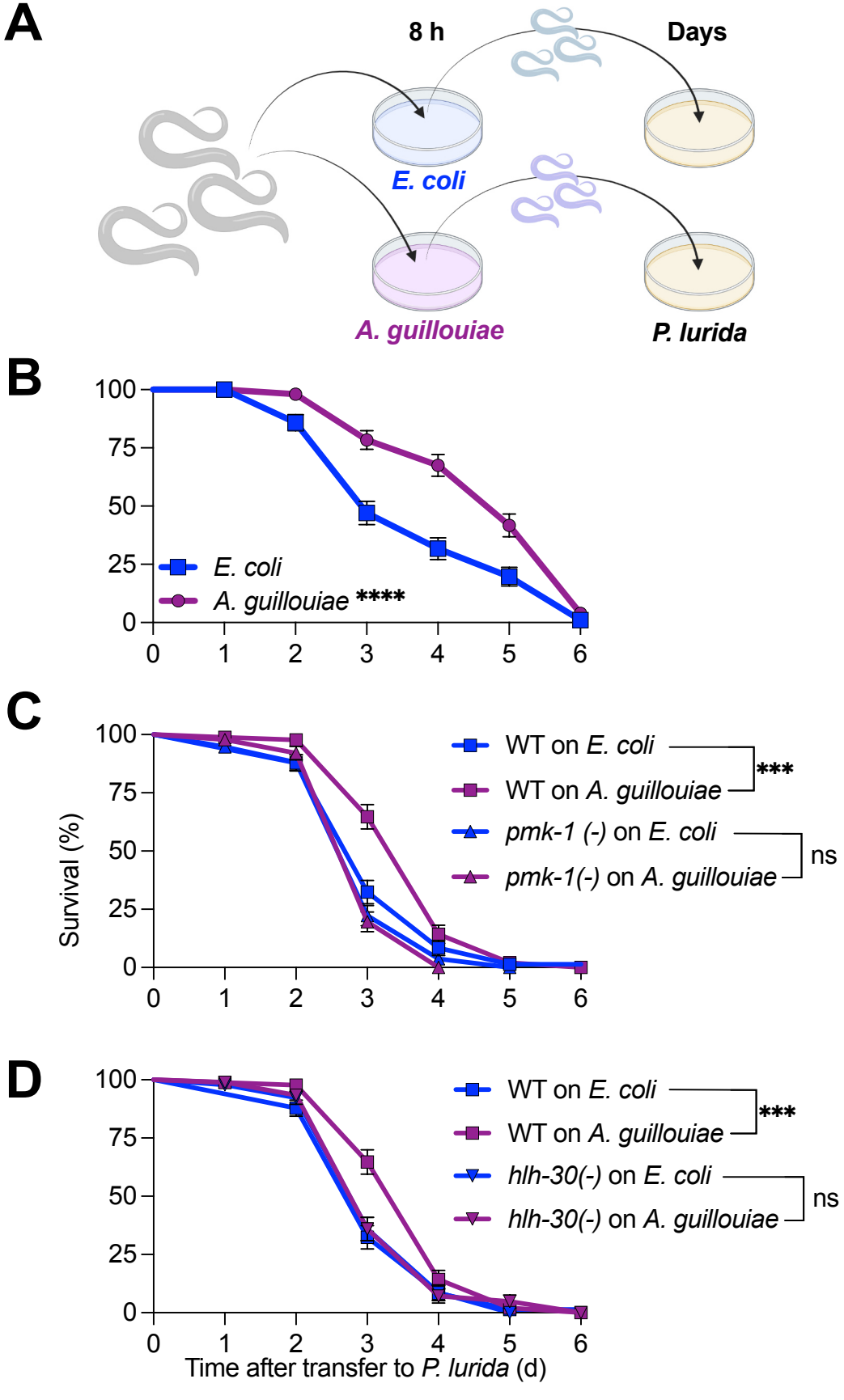

Gonzalez et al Figure 8